Optical absorption modulation by selective codoping of SiGe core-shell nanowires

Michele Amato, Maurizia Palummo, Riccardo Rurali, and Stefano Ossicini

Additional information on J. Appl. Phys.

Optical absorption modulation by selective codoping of SiGe core-shell nanowires

Michele Amato,[1] Maurizia Palummo,[2] Riccardo Rurali,[3] and Stefano Ossicini[4,5,6,a]

[1]*Laboratoire de Physique des Solides (LPS), Université Paris Sud, CNRS UMR 8502, F-91405 Orsay, France*
[2]*Dipartimento di Fisica, CNISM, ETSF Università di Roma, "Tor Vergata", Via della Ricerca Scientifica 1, 00133 Roma, Italy*
[3]*Institut de Ciència de Materials de Barcelona (ICMAB-CSIC), Campus de Bellaterra, 08193 Bellaterra, Barcelona, Spain*
[4]*"Centro S³," CNR-Istituto di Nanoscienze, Via Campi 213/A, 41125 Modena, Italy*
[5]*Dipartimento di Scienze e Metodi dell'Ingegneria, Universitá di Modena e Reggio Emilia, Via Amendola 2 Pad. Morselli, I-41122 Reggio Emilia, Italy*
[6]*Centro Interdipartimentale En&Tech, Universitá di Modena e Reggio Emilia, Via Amendola 2 Pad. Morselli, I-41122 Reggio Emilia, Italy*

First-principles calculations on the structural, electronic, and optical properties of B-P codoped SiGe core-shell nanowires are discussed. We show that the simultaneous addition of B and P impurities into the wire can be energetically favored with respect to the single-doping. We demonstrate that impurities energetic levels in the band gap are dependent by the Si/Ge band offset, as well as by their location in the wire (i.e., core or shell region). This electronic tunability results in a significant optical modulation, as demonstrated by the red-shift of the first optical peak when B and P locations are switched in the wire. © 2012 American Institute of Physics. [http://dx.doi.org/10.1063/1.4768475]

The vision of Si nanoelectronics, which uses Si nanostructures[1–4] as building blocks, is to design and engineer new materials and devices that will overcome Moore's law limits.[5] In this context, the understanding of the role of intentional addition of impurities in nanostructures can be of paramount importance for further developments in the field. Doping has been the corner-stone of Si microelectronics and now, thanks to major progresses in chemical synthesis and materials processing, is playing a crucial role also in nanoscience. Numerous works[2,6–9] have shown that the single or simultaneous addition of group III-V impurities—like B or P—in a pure Si nanomaterial modifies its electronic structure, enhancing charge carriers concentration and electrical mobility. In particular, in the last years, codoped Si nanocrystals (NCs) and nanowires (NWs)[6,7,10–14] have been the subject of intense theoretical and experimental studies, which pave the way to very intriguing and exciting technological applications in the field of optoelectronics, high performance nanoelectronics, thermoelectrics, and photovoltaics. For example, Fujii *et al.*[6] have demonstrated that the simultaneous addition of B and P impurities in Si NCs leads to an improvement of the photoluminescence efficiency.

Here, we discuss the structural, electronic, and optical properties of codoped SiGe core-shell nanowires. The enormous interest towards these systems has been originally motivated by their unique properties, such as ease of processing, compatibility with existent Si technology, electronic and optical features that can be tuned by size, chemical composition, and geometry of Si/Ge interface. Recently, important advances in modeling, synthesis, and device engineering[15–18] have enabled the fabrication of SiGe core-shell devices with improved performance and reproducibility. Following we show that by playing with type II Si/Ge band offset[19,20] and with the impurity location in the wire, a remarkable modulation of the low energy optical peaks can be achieved. Additionally, by evaluating the impurity formation energy (FE), we attempt to describe how simultaneous codoping can affect the impurity solubility with respect to the single doped case. To date, very few theoretical studies have addressed the question of the single-doping of core-shell SiGe NWs[21–23] and no studies have been dedicated to codoping.

We have carried out the theoretical investigation of these systems by means of *ab-initio* calculations in the framework of density functional theory (DFT). Ge_{core}/Si_{shell} NWs oriented along the [110] direction and with diameter $d = 2.4$ nm have been studied; B and P have been considered as substitutional impurities in both core and shell lattice sites. As core site, we have chosen the lattice site centered in the cross section of the wire, while a shell site means a subsurface lattice one (see Fig. 1). Moreover, the two impurities are placed along the direction of growth of the wire in order to maximize their relative distance (nearly 17 Å) that means they do not belong to the same lattice planes. This is done in order to ensure that the results do not depend upon dopant-dopant interaction. The impurity concentration in our wires is comparable with the high-doping regime values of several experimental studies on pure and alloyed NWs.[24,25] We have analyzed pristine Ge_{core}/Si_{shell} NWs, B-doped-Ge_{core}/P-doped-Si_{shell} (p-$type_{core}$/n-$type_{shell}$) and P-doped-Ge_{core}/B-doped-Si_{shell} (n-$type_{core}$/p-$type_{shell}$) NWs. The geometry of the considered wires is the same of Ref. 22. For all the considered NWs, a full geometry optimization (both atomic positions and cell parameters) through the Broyden-Fletcher-Goldfarb-Shanno technique[26] has been performed with a

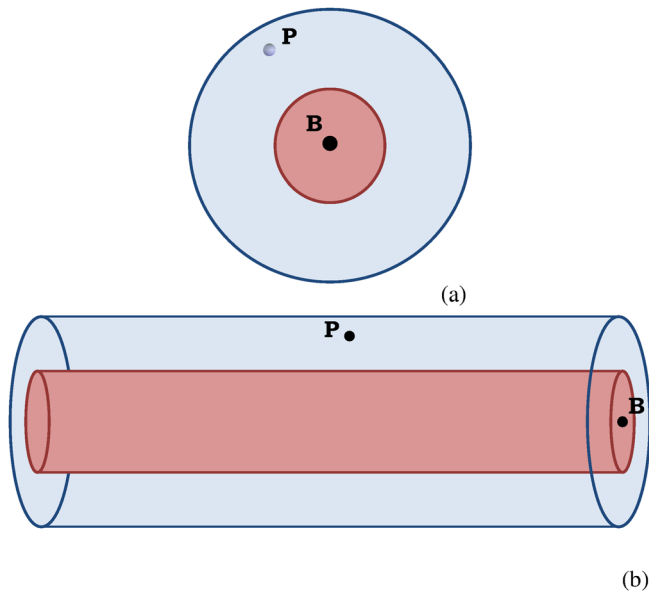a)Electronic mail: stefano.ossicini@unimore.it.

FIG. 1. Top (a) and side (b) view of a codoped p-type core/n-type shell core-shell NWs.

maximum force tolerance of 0.04 eV/Å. Supercells made of six primitive cells have been built in order to eliminate the spurious interaction between periodic images of impurities. For such large computational supercells, only one k-point along the periodic direction of the system, i.e., the axial direction, is sufficient to achieve accurate structural relaxations. No sampling of the Brillouin zone along the transversal directions is required, because the system is not periodic in those directions. Upon recalculation the electronic structure with a $1 \times 1 \times 16$ k-point grid, however, we found that the forces were still within the tolerance limits established for the structural relaxation and range from 0.018 to 0.031 eV/Å (the maximum force tolerance being 0.04 eV/Å), justifying the Γ point relaxations.

All the calculations have been performed in the framework of DFT for the ground state study and of the random-phase-approximation for the optical properties, as implemented in the plane-waves code Quantum Espresso.[27] Local density approximation (LDA) has been chosen for the exchange-correlation functional. An energy cutoff to 30 Ry and the same norm-conserving pseudo potentials of Ref. [28] have been used. Differently from that work, here we are obliged to build a very large supercell along the axial direction, with more than 700 atoms. This is done to eliminate the spurious interaction between periodic images of impurities and to reproduce experimental impurity concentrations. As is well known, in principle, only many-body perturbation theory (MBPT) calculations on top of DFT ones could provide a proper description of electronic and optical properties,[29] taking into account self-energy and excitonic effects. Nevertheless, this kind of *first-principles* excited-state calculations is completely unfeasible in our case due to the large number of atoms in the simulation cell. Indeed, the calculation of the quasi-particle energies with the GW approach and of the dielectric response by solving the Bethe-Salpeter equation (which takes into account the electron-hole interaction) is

very cumbersome and is now limited to systems with up to few hundred of atoms. It is also worth to underline that in nanostructures these effects very often nearly cancel each other, making LDA estimates about the optical energy-band-gap still reasonably valid.[30–33] We are then convinced that the present work can provide a first, qualitatively correct, description of the optical properties of these SiGe codoped nanowires. Furthermore, in a previous work,[34] we explicitly calculated the GW corrections for pure SiGe core-shell NWs showing that they can be obtained as a weighted average, on the relative atomic composition, of the corrections of pure Si and Ge nanowire of the same diameter. Though we cannot state that this rule is valid also in the case of the codoped wire, we refer the reader to that work[34] to have an idea of the numerical error of the LDA results with respect to the real electronic gaps of these one-dimensional nanostructures.

Structural Stability: As a first step, we attempt to describe the energetic stability of both single-doped and codoped NWs calculating their FE that is the cost in energy of creating a defect in the host material. The FE has been evaluated using the formalism of Ref. [22], especially developed for core-shell NWs. Results of FE calculations are reported in Fig. 2 (corresponding numerical values of the graph are listed in Tables I and II). In the case of single doping (see Table I), in accordance with the previous works on pure NWs,[11] impurities show a moderate tendency to occupy surface sites of the wire and impurities in the shell sites have the lowest FE. On the other hand, looking at the FE values of codoped wires (see first column of Table II), it is clear that $n\text{-}type_{core}/p\text{-}type_{shell}$ configuration is stable with respect to the $p\text{-}type_{core}/n\text{-}type_{shell}$ one. The comparison between FE of a single-doped and a codoped case can be done by correlating the FE a codoped wire with the sum of FEs of the
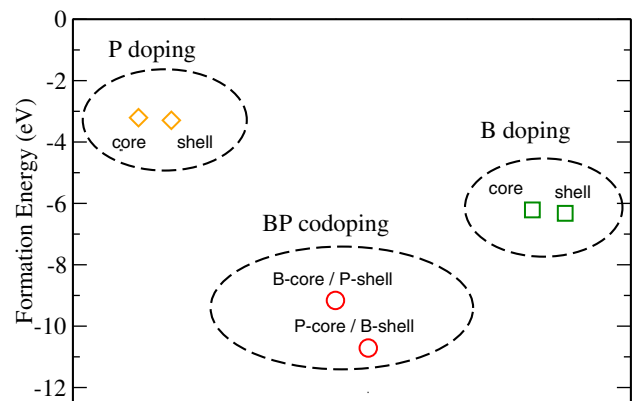

FIG. 2. Formation energies of the impurities as a function of the location in the wire (core or shell) and the type of doping (n-type or p-type).

TABLE I. Formation energies (eV) of P (top row) and B (bottom row) single substitutionals in the core (first column) and shell (second column) of single-doped Ge_{core}/Si_{shell} NWs.

	Core	Shell
n-type	−3.20	−3.29
p-type	−6.21	−6.32

TABLE II. Formation energies (eV) of P and B for codoped (first column) n-type$_{core}$/p-type$_{shell}$ (first row) and p-type$_{core}$/n-type$_{shell}$ (second row) Ge$_{core}$/Si$_{shell}$ NWs. Comparison with the sum of FEs of the corresponding single-doping configurations is presented in the second column.

	Co-doped	Sum of single-doped
n-type$_{core}$/p-type$_{shell}$	−10.72	−9.52
p-type$_{core}$/n-type$_{shell}$	−9.16	−9.50

corresponding single-doping configurations (reported in the second column of Table II). In this way, one compares energy values derived from the same number of impurity substitutions. Our results obtained in this assumption reveal that while for the *p-type$_{core}$/n-type$_{shell}$* wire the codoping gives FE values similar to that evaluated as a sum of the corresponding single-doping FEs, for the *n-type$_{core}$/p-type$_{shell}$* configuration codoping results in a gain of energy with respect to the corresponding single-doped case, with a FE that is more than 1 eV lower. This behavior has been ascribed, in the case of codoped Si NCs and NWs, to both charge compensation and minor structural deformation.[7,11]

Electronic structure: We preliminarily focus our analysis on the electronic structure of undoped Ge$_{core}$/Si$_{shell}$ NWs. In agreement with the previous report,[22] in an undoped core-shell NW, the presence of a Si/Ge interface gives rise to a type II band offset between the two materials.[19] This particular band alignment implies that the maximum of the valence band is completely localized on the Ge part of the wire, while the minimum of conduction band is strongly localized on Si (see the sketches in Fig. 3). The type II band offset represents a general property of SiGe systems, which has been found in different types of novel nanostructures[20,35] as well as deeply studied in other SiGe materials.[19,36,37]

Next, we analyze the effect of BP codoping on the electronic structure of core-shell NWs. As already demonstrated in a previous study,[22] by single-doping of SiGe core-shell NWs, it is possible to obtain a one-dimensional electron (hole) gas, remarkably increasing the doping efficiency. This is not the case of codoped core-shell NWs where the simultaneous addition of acceptor and donor impurities completely compensate the whole charge of the system, avoiding the creation of any type of charge carrier gas. Interestingly, however, here we show that switching the dopant species between core and shell, profoundly changes the electronic transitions, inducing a noticeable shift in the first absorption
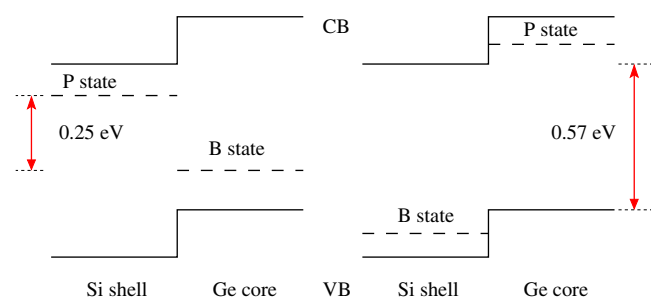

FIG. 3. Energy levels diagram for *p-type$_{core}$/n-type$_{shell}$* NWs (left panel) and *n-type$_{core}$/p-type$_{shell}$* NWs (right panel). The graph is not in scale.

peak. We start by considering a simultaneous B substitution in the Ge core and P substitution in the Si shell (*p-type$_{core}$/n-type$_{shell}$* configuration). In this case (see left panel of Fig. 3), the energetic level position of both impurities falls deep inside into the band gap, as clearly demonstrated for other codoped nanostructures.[7,10,13] An analysis of the electronic wave function localization (not shown here) indicates that B (P) state is localized a few hundredths of meV above (below) the top (bottom) of the valence (conduction) band. Hence, in this configuration, the electronic structure is strongly changed with respect to the pure case due to the presence of donor and acceptor states into the band gap.

On the other hand, switching the codoping configuration, i.e., substituting a Ge core atom with P and a Si shell atom with B (*n-type$_{core}$/p-type$_{shell}$* configuration) does not result in any modification of the electronic structure with respect to the undoped case. In this configuration, the codoping mechanism can be easily understood by the band offset picture sketched in the right panel of Fig. 3. Calculations of the spatial wave function localizations (not shown here) indicate that B (P) impurity state lies deep into the valence (conduction) band, keeping the electronic structure unaltered with respect to the undoped wire. The physical origin of this effect is related to the type II band offset: due to quantum and dielectric confinement, in a pure Ge NW, the impurity state would be deep into the band gap.[38] In a core-shell wire, putting a single acceptor (donor) atom on Si (Ge) part of the wire results in an impurity state deep into the valence (conduction) bands, because the top of valence (conduction) band is completely located on Ge (Si) as a consequence of the type II band alignment.[22] Hence, in this case of codoping, the simultaneous addition of an acceptor on Si and a donor on Ge makes impurities states falling down deep into electronic and holes bands, avoiding any modification of the energy level diagram with respect to the undoped wire (see right panel of Fig. 3). For sake of clarity, we have focused our analysis on Ge$_{core}$/Si$_{shell}$ NWs; however, the same type of discussion, with the appropriate differences, can be also applied in the case of Si$_{core}$/Ge$_{shell}$ NWs.

Optical Spectra: The tunability of electronic structure offers an easy way to modulate the optical spectra. In Fig. 4, results of calculations of the optical absorption spectra are reported for pristine Ge$_{core}$/Si$_{shell}$, *n-type$_{core}$/p-type$_{shell}$*, and *p-type$_{core}$/n-type$_{shell}$* NWs. From the figure, it is clear that the optical spectrum does not change significantly with respect to the undoped NW, when the Ge core is n-type doped and the Si shell is p-type. On the other hand, switching the impurities location into the wire, i.e., putting a B in the Ge core and a P atom in Si shell, results in a strong red-shift of the lowest energy optical peak, direct consequence of the presence of donor-acceptor transition. From the analysis of spatial localization of electronic states (not shown here), we confirm that the first peak of the orange curve of Fig. 4 corresponds to a B-P transition, while the first peaks of the other two spectra (black and red curves) correspond to Ge/Si transitions.

In conclusion, by means of first-principles calculations, we have demonstrated that the simultaneous addition B and P impurities in Ge$_{core}$/Si$_{shell}$ NWs can result in a gain of energy with respect to the single-doping cases. Furthermore,

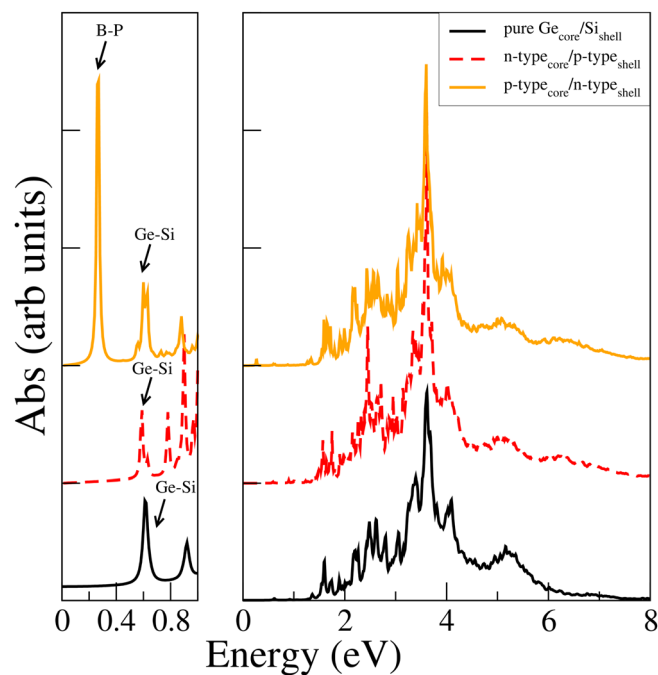FIG. 4. Right panel: Absorption spectra of undoped Ge$_{core}$/Si$_{shell}$ NWs (black solid line), *n-type$_{core}$/p-type$_{shell}$* NWs (red/dark gray dashed curve), and *p-type$_{core}$/n-type$_{shell}$* NWs (orange/light gray solid line). Left panel: low-energy part zoom. The arrows indicate the onset of optical spectra and the type of transition.

we have shown and discussed that a noticeable modulation of electronic transitions and optical peaks at the onset of the absorption spectrum can be reached by switching location of impurities in the wire. Since so far no studies have been dedicated to the optical absorption of codoped SiGe NWs, unfortunately we cannot compare our results with experimental data. Nevertheless, we strongly believe that these findings suggest a promising way to engineer light absorption in nanowires, which can be crucial in designing and modeling opto-electronic nanowire-based devices.

[1] O. Bisi, S. Ossicini, and L. Pavesi, Surf. Sci. Rep. **38**, 1 (2000).
[2] S. G. Pavlov, R. Eichholz, N. V. Abrosimov, B. Redlich, and H.-W. Hubers, Appl. Phys. Lett. **98**, 061102 (2011).
[3] L. T. Canham, Appl. Phys. Lett. **57**, 1046 (1990).
[4] R. Rurali, Rev. Mod. Phys. **82**, 427 (2010).
[5] S. E. Thompson and S. Parthasarathy, Mater. Today **9**, 20 (2006).
[6] M. Fujii, Y. Yamaguchi, Y. Takase, K. Ninomiya, and S. Hayashi, Appl. Phys. Lett. **85**, 1158 (2004).
[7] S. Ossicini, E. Degoli, F. Iori, E. Luppi, R. Magri, G. Cantele, F. Trani, and D. Ninno, Appl. Phys. Lett. **87**, 173120 (2005).
[8] J. Nah, K. Varahramyan, E.-S. Liu, S. K. Banerjee, and E. Tutuc, Appl. Phys. Lett. **93**, 203108 (2008).
[9] N. Fukata, Adv. Mater. **21**, 2829 (2009).
[10] H. Peelaers, B. Partoens, and F. M. Peeters, Appl. Phys. Lett. **90**, 263103 (2007).
[11] H. Peelaers, B. Partoens, and F. M. Peeters, Nano Lett. **6**, 2781 (2006).
[12] N. Fukata, M. Mitome, Y. Bando, M. Seoka, S. Matsushita, K. Murakami, J. Chen, and T. Sekiguchi, Appl. Phys. Lett. **93**, 203106 (2008).
[13] M. Palummo, F. Iori, R. D. Sole, and S. Ossicini, Superlattice Microstruct. **46**, 234 (2009).
[14] N. Fukata, J. Chen, T. Sekiguchi, S. Matsushita, T. Oshima, N. Uchida, K. Murakami, T. Tsurui, and S. Ito, Appl. Phys. Lett. **90**, 153117 (2007).
[15] L. J. Lauhon, M. S. Gudiksen, D. Wang, and C. M. Lieber, Nature **420**, 57 (2002).
[16] W. Lu, J. Xiang, B. P. Timko, Y. Wu, and C. M. Lieber, Proc. Natl. Acad. Sci. U.S.A. **102**, 10046 (2005).
[17] G. Liang, J. Xiang, N. Kharche, G. Klimeck, C. M. Lieber, and M. Lundstrom, Nano Lett. **7**, 642 (2007).
[18] W. Y. Fung, L. Chen, and W. Lu, Appl. Phys. Lett. **99**, 092108 (2011).
[19] C. Van de Walle and R. Martin, Phys. Rev. B **35**, 8154 (1987).
[20] S. Huang and L. Yang, Appl. Phys. Lett. **98**, 093114 (2011).
[21] A. Nduwimana and X.-Q. Wang, Nano Lett. **9**, 283 (2009).
[22] M. Amato, S. Ossicini, and R. Rurali, Nano Lett. **11**, 594 (2011).
[23] H. Lee and H. J. Choi, Nano Lett. **10**, 2207 (2010).
[24] J. Nah, E.-S. Liu, D. Shahrjerdi, K. M. Varahramyan, S. K. Banerjee, and E. Tutuc, Appl. Phys. Lett. **94**, 063117 (2009).
[25] Y. Wang, K.-K. Lew, T.-T. Ho, L. Pan, S. W. Novak, E. C. Dickey, J. M. Redwing, and T. S. Mayer, Nano Lett. **5**, 2139 (2005).
[26] A. Mordecai, *Nonlinear Programming: Analysis and Methods* (Dover, New York, 2003).
[27] P. Giannozzi, S. Baroni, N. Bonini, M. Calandra, R. Car, C. Cavazzoni, D. Ceresoli, G. L. Chiarotti, M. Cococcioni, I. Dabo, A. D. Corso, S. de Gironcoli, S. Fabris, G. Fratesi, R. Gebauer, U. Gerstmann, C. Gougoussis, A. Kokalj, M. Lazzeri, L. Martin-Samos, N. Marzari, F. Mauri, R. Mazzarello, S. Paolini, A. Pasquarello, L. Paulatto, C. Sbraccia, S. Scandolo, G. Sclauzero, A. P. Seitsonen, A. Smogunov, P. Umari, and R. M. Wentzcovitch, J. Phys.: Condens. Matter **21**, 395502 (2009).
[28] M. Amato, M. Palummo, and S. Ossicini, Phys. Rev. B **80**, 235333 (2009).
[29] G. Onida, L. Reining, and A. Rubio, Rev. Mod. Phys. **74**, 601 (2002).
[30] K. Frey, J. C. Idrobo, M. L. Tiago, F. Reboredo, and S. Öğüt, Phys. Rev. B **80**, 153411 (2009).
[31] M. Bruno, M. Palummo, A. Marini, R. Del Sole, V. Olevano, A. N. Kholod, and S. Ossicini, Phys. Rev. B **72**, 153310 (2005).
[32] L. Yang, J. Deslippe, C.-H. Park, M. L. Cohen, and S. G. Louie, Phys. Rev. Lett. **103**, 186802 (2009).
[33] M. Bernardi, M. Palummo, and J. C. Grossman, Phys. Rev. Lett. **108**, 226805 (2012).
[34] M. Palummo, M. Amato, and S. Ossicini, Phys. Rev. B **82**, 073305 (2010).
[35] A. Nduwimana, R. N. Musin, A. M. Smith, and X.-Q. Wang, Nano Lett. **8**, 3341 (2008).
[36] S. Ciraci and I. P. Batra, Phys. Rev. B **38**, 1835 (1988).
[37] D. J. Paul, Thin Solid Films **321**, 172 (1998).
[38] M. T. Björk, H. Schmid, J. Knoch, H. Riel, and W. Riess, Nat. Nanotechnol. **4**, 103 (2009).